

Measurement of the e^+e^- Invariant-Mass Distribution in $\bar{p}p$ Collisions at $\sqrt{s} = 1.8$ TeV

F. Abe,⁽⁹⁾ D. Amidei,⁽⁴⁾ G. Apollinari,⁽¹⁵⁾ M. Atac,⁽⁴⁾ P. Auchincloss,⁽¹⁴⁾ A. R. Baden,⁽⁶⁾ M. Bailey,⁽¹³⁾ A. Bamberger,^{(4),(a)} B. A. Barnett,⁽⁸⁾ A. Barbaro-Galtieri,⁽¹⁰⁾ V. E. Barnes,⁽¹³⁾ T. Baumann,⁽⁶⁾ F. Bedeschi,⁽¹²⁾ S. Behrens,⁽²⁾ S. Belforte,⁽¹²⁾ G. Bellettini,⁽¹²⁾ J. Bellinger,⁽²⁰⁾ J. Bensingler,⁽²⁾ A. Beretvas,⁽⁴⁾ J. P. Berge,⁽⁴⁾ S. Bertolucci,⁽⁵⁾ S. Bhadra,⁽⁷⁾ M. Binkley,⁽⁴⁾ R. Blair,⁽¹⁾ C. Blocker,⁽²⁾ V. Bolognesi,⁽¹²⁾ A. W. Booth,⁽⁴⁾ C. Boswell,⁽⁸⁾ G. Brandenburg,⁽⁶⁾ D. Brown,⁽⁶⁾ E. Buckley-Geer,⁽¹⁶⁾ H. S. Budd,⁽¹⁴⁾ A. Byon,⁽¹³⁾ K. L. Byrum,⁽²⁰⁾ C. Campagnari,⁽³⁾ M. Campbell,⁽³⁾ R. Carey,⁽⁶⁾ W. Carithers,⁽¹⁰⁾ D. Carlsmith,⁽²⁰⁾ J. T. Carroll,⁽⁴⁾ R. Cashmore,^{(4),(a)} F. Cervelli,⁽¹²⁾ K. Chadwick,⁽⁴⁾ G. Chiarelli,⁽⁵⁾ W. Chinowsky,⁽¹⁰⁾ S. Cihangir,⁽⁴⁾ A. G. Clark,⁽⁴⁾ D. Connor,⁽¹¹⁾ M. Contreras,⁽²⁾ J. Cooper,⁽⁴⁾ M. Cordelli,⁽⁵⁾ D. Crane,⁽⁴⁾ M. Curatolo,⁽⁵⁾ C. Day,⁽⁴⁾ S. Dell'Agnello,⁽¹²⁾ M. Dell'Orso,⁽¹²⁾ L. Demortier,⁽²⁾ P. F. Derwent,⁽³⁾ T. Devlin,⁽¹⁶⁾ D. DiBitonto,⁽¹⁷⁾ R. B. Drucker,⁽¹⁰⁾ J. E. Elias,⁽⁴⁾ R. Ely,⁽¹⁰⁾ S. Eno,⁽³⁾ S. Errede,⁽⁷⁾ B. Esposito,⁽⁵⁾ B. Flaughner,⁽⁴⁾ G. W. Foster,⁽⁴⁾ M. Franklin,⁽⁶⁾ J. Freeman,⁽⁴⁾ H. Frisch,⁽³⁾ T. Fuess,⁽⁴⁾ Y. Fukui,⁽⁹⁾ Y. Funayama,⁽¹⁸⁾ A. F. Garfinkel,⁽¹³⁾ A. Gauthier,⁽⁷⁾ S. Geer,⁽⁴⁾ P. Giannetti,⁽¹²⁾ N. Giokaris,⁽¹⁵⁾ P. Giromini,⁽⁵⁾ L. Gladney,⁽¹¹⁾ M. Gold,⁽¹⁰⁾ K. Goulianos,⁽¹⁵⁾ H. Grassmann,⁽¹²⁾ C. Grosso-Pilcher,⁽³⁾ C. Haber,⁽¹⁰⁾ S. R. Hahn,⁽⁴⁾ R. Handler,⁽²⁰⁾ K. Hara,⁽¹⁸⁾ R. M. Harris,⁽⁴⁾ J. Hauser,⁽⁴⁾ C. Hawk,⁽¹⁶⁾ T. Hessing,⁽¹⁷⁾ R. Hollebeek,⁽¹¹⁾ L. Holloway,⁽⁷⁾ P. Hu,⁽¹⁶⁾ B. Hubbard,⁽¹⁰⁾ B. T. Huffman,⁽¹³⁾ R. Hughes,⁽¹¹⁾ P. Hurst,⁽⁵⁾ J. Huth,⁽⁴⁾ M. Incagli,⁽¹²⁾ T. Ino,⁽¹⁸⁾ H. Iso,⁽¹⁸⁾ H. Jensen,⁽⁴⁾ C. P. Jessop,⁽⁶⁾ R. P. Johnson,⁽⁴⁾ U. Joshi,⁽⁴⁾ R. W. Kadel,⁽¹⁰⁾ T. Kamon,⁽¹⁷⁾ S. Kanda,⁽¹⁸⁾ D. A. Kardelis,⁽⁷⁾ I. Karliner,⁽⁷⁾ E. Kearns,⁽⁶⁾ L. Keeble,⁽¹⁷⁾ R. Kephart,⁽⁴⁾ P. Kesten,⁽²⁾ R. M. Keup,⁽⁷⁾ H. Keutelian,⁽⁴⁾ D. Kim,⁽⁴⁾ S. Kim,⁽¹⁸⁾ L. Kirsch,⁽²⁾ K. Kondo,⁽¹⁸⁾ J. Konigsberg,⁽⁶⁾ E. Kovacs,⁽⁴⁾ S. E. Kuhlmann,⁽¹⁾ E. Kuns,⁽¹⁶⁾ A. T. Laasanen,⁽¹³⁾ J. I. Lamoureux,⁽²⁰⁾ S. Leone,⁽¹²⁾ W. Li,⁽¹⁾ T. M. Liss,⁽⁷⁾ N. Lockyer,⁽¹¹⁾ C. B. Luchini,⁽⁷⁾ P. Maas,⁽²⁾ K. Maeshima,⁽⁴⁾ M. Mangano,⁽¹²⁾ J. P. Marriner,⁽⁴⁾ R. Markeloff,⁽²⁰⁾ L. A. Markosky,⁽²⁰⁾ R. Mattingly,⁽²⁾ P. McIntyre,⁽¹⁷⁾ A. Menzione,⁽¹²⁾ T. Meyer,⁽¹⁷⁾ S. Mikamo,⁽⁹⁾ M. Miller,⁽³⁾ T. Mimashi,⁽¹⁸⁾ S. Miscetti,⁽⁵⁾ M. Mishina,⁽⁹⁾ S. Miyashita,⁽¹⁸⁾ Y. Morita,⁽¹⁸⁾ S. Moulding,⁽²⁾ J. Mueller,⁽¹⁶⁾ A. Mukherjee,⁽⁴⁾ L. F. Nakae,⁽²⁾ I. Nakano,⁽¹⁸⁾ C. Nelson,⁽⁴⁾ C. Newman-Holmes,⁽⁴⁾ J. S. T. Ng,⁽⁶⁾ M. Ninomiya,⁽¹⁸⁾ L. Nodulman,⁽¹⁾ S. Ogawa,⁽¹⁸⁾ R. Paoletti,⁽¹²⁾ A. Para,⁽⁴⁾ E. Pare,⁽⁶⁾ J. Patrick,⁽⁴⁾ T. J. Phillips,⁽⁶⁾ R. Plunkett,⁽⁴⁾ L. Pondrom,⁽²⁰⁾ J. Proudfoot,⁽¹⁾ G. Punzi,⁽¹²⁾ D. Quarrie,⁽⁴⁾ K. Ragan,⁽¹¹⁾ G. Redlinger,⁽³⁾ J. Rhoades,⁽²⁰⁾ M. Roach,⁽¹⁹⁾ F. Rimondi,^{(4),(a)} L. Ristori,⁽¹²⁾ T. Rohaly,⁽¹¹⁾ A. Roodman,⁽³⁾ W. K. Sakumoto,⁽¹⁴⁾ A. Sansoni,⁽⁵⁾ R. D. Sard,⁽⁷⁾ A. Savoy-Navarro,⁽⁴⁾ V. Scarpine,⁽⁷⁾ P. Schlabach,⁽⁷⁾ E. E. Schmidt,⁽⁴⁾ M. H. Schub,⁽¹³⁾ R. Schwitters,⁽⁶⁾ A. Scribano,⁽¹²⁾ S. Segler,⁽⁴⁾ Y. Seiya,⁽¹⁸⁾ M. Sekiguchi,⁽¹⁸⁾ M. Shapiro,⁽¹⁰⁾ N. M. Shaw,⁽¹³⁾ M. Sheaff,⁽²⁰⁾ M. Shochet,⁽³⁾ J. Siegrist,⁽¹⁰⁾ P. Sinervo,⁽¹¹⁾ J. Skarha,⁽⁸⁾ K. Sliwa,⁽¹⁹⁾ D. A. Smith,⁽¹²⁾ F. D. Snider,⁽⁸⁾ L. Song,⁽¹¹⁾ R. St. Denis,⁽⁶⁾ A. Stefanini,⁽¹²⁾ G. Sullivan,⁽³⁾ R. L. Swartz, Jr.,⁽⁷⁾ M. Takano,⁽¹⁸⁾ F. Tartarelli,⁽¹²⁾ K. Takikawa,⁽¹⁸⁾ S. Tarem,⁽²⁾ D. Theriot,⁽⁴⁾ M. Timko,⁽¹⁷⁾ P. Tipton,⁽⁴⁾ S. Tkaczyk,⁽⁴⁾ A. Tollestrup,⁽⁴⁾ J. Tonnison,⁽¹³⁾ W. Trischuk,⁽⁶⁾ Y. Tsay,⁽³⁾ F. Ukegawa,⁽¹⁸⁾ D. Underwood,⁽¹⁾ S. Vejckic, III,⁽⁸⁾ R. Vidal,⁽⁴⁾ R. G. Wagner,⁽¹⁾ R. L. Wagner,⁽⁴⁾ N. Wainer,⁽⁴⁾ J. Walsh,⁽¹¹⁾ T. Watts,⁽¹⁶⁾ R. Webb,⁽¹⁷⁾ C. Wendt,⁽²⁰⁾ W. C. Wester, III,⁽¹⁰⁾ T. Westhusing,⁽¹²⁾ S. N. White,⁽¹⁵⁾ A. B. Wicklund,⁽¹⁾ H. H. Williams,⁽¹¹⁾ B. L. Winer,⁽¹⁰⁾ A. Yagil,⁽⁴⁾ A. Yamashita,⁽¹⁸⁾ K. Yasuoka,⁽¹⁸⁾ G. P. Yeh,⁽⁴⁾ J. Yoh,⁽⁴⁾ M. Yokoyama,⁽¹⁸⁾ J. C. Yun,⁽⁴⁾ and F. Zetti⁽¹²⁾

(CDF Collaboration)

⁽¹⁾Argonne National Laboratory, Argonne, Illinois 60439

⁽²⁾Brandeis University, Waltham, Massachusetts 02254

⁽³⁾University of Chicago, Chicago, Illinois 60637

⁽⁴⁾Fermi National Accelerator Laboratory, Batavia, Illinois 60510

⁽⁵⁾Laboratori Nazionali di Frascati, Istituto Nazionale di Fisica Nucleare, Frascati, Italy

⁽⁶⁾Harvard University, Cambridge, Massachusetts 02138

⁽⁷⁾University of Illinois, Urbana, Illinois 61801

⁽⁸⁾The Johns Hopkins University, Baltimore, Maryland 21218

⁽⁹⁾National Laboratory for High Energy Physics (KEK), Tsukuba, Ibaraki 305, Japan

⁽¹⁰⁾Lawrence Berkeley Laboratory, Berkeley, California 94720

⁽¹¹⁾University of Pennsylvania, Philadelphia, Pennsylvania 19104

⁽¹²⁾Istituto Nazionale di Fisica Nucleare, University and Scuola Normale Superiore of Pisa, I-56100 Pisa, Italy

⁽¹³⁾*Purdue University, West Lafayette, Indiana 47907*

⁽¹⁴⁾*University of Rochester, Rochester, New York 14627*

⁽¹⁵⁾*Rockefeller University, New York, New York 10021*

⁽¹⁶⁾*Rutgers University, Piscataway, New Jersey 08854*

⁽¹⁷⁾*Texas A&M University, College Station, Texas 77843*

⁽¹⁸⁾*University of Tsukuba, Tsukuba, Ibaraki 305, Japan*

⁽¹⁹⁾*Tufts University, Medford, Massachusetts 02155*

⁽²⁰⁾*University of Wisconsin, Madison, Wisconsin 53706*

(Received 16 July 1991)

We have measured the cross section as a function of invariant mass for isolated electron pairs produced in $\bar{p}p$ collisions at $\sqrt{s} = 1.8$ TeV for pair masses $M > 30$ GeV/ c^2 . We find good agreement between the measured distribution and the standard-model prediction for the Drell-Yan production mechanism. Additional heavy neutral vector bosons (Z') are excluded for $M_{Z'} < 387$ GeV/ c^2 (95% confidence level) assuming standard-model couplings. A lower limit of 2.2 TeV (95% confidence level) is placed on the electron-quark compositeness scale parameter $\Lambda_{\bar{L}\bar{L}}$ associated with an effective contact interaction.

PACS numbers: 13.85.Qk, 12.15.Cc, 12.50.Ch, 13.85.Rm

We present a measurement of the electron-pair-production cross section in $\bar{p}p$ collisions at $\sqrt{s} = 1.8$ TeV for pair masses $M > 30$ GeV/ c^2 . In the parton model, isolated lepton pairs are produced in $\bar{p}p$ collisions by the Drell-Yan mechanism [1]. The cross section is a convolution of parton distribution functions and the subprocess cross section at the effective center-of-mass energy \hat{s} . In the standard model, this subprocess is the result of either virtual photon or real or virtual Z production. For the mass range of this measurement the cross section is dominated by the Z resonance. For low pair masses the cross section rises due to virtual photon production. At sufficiently low masses (outside the scope of this analysis) the distribution is expected to be sensitive to the parton distribution functions [2]. Above the Z resonance the cross section is expected to fall off rapidly due to the $1/\hat{s}$ behavior of the virtual boson propagator, thereby providing a window on phenomena outside the standard model. In particular, additional neutral vector bosons are expected in many extensions of the standard model [3]. Such bosons would be directly observed as additional resonances in this distribution. In addition, a flattening of the cross section at high mass (above the Z) is expected in composite models where leptons and quarks share constituents [4].

The data presented here were collected with the Collider Detector at Fermilab (CDF), corresponding to an integrated luminosity of 4.05 pb^{-1} . We summarize the essential features of the CDF relevant to this analysis [5]. Planes of scintillation (beam-beam) counters located at small angles to the beam signal an inelastic $\bar{p}p$ collision. Vertex time projection chambers (VTPC) provide a measurement of the event vertex as well as tracking information out to a radius of 22 cm from the beam axis and cover the pseudorapidity range $|\eta| < 3.5$ [$\eta \equiv -\ln \tan(\theta/2)$, where θ is the polar angle with respect to the proton beam]. At larger radii, an 84-layer central tracking chamber (CTC) immersed in a 1.4-T magnetic field provides tracking with high efficiency and measures momenta with a precision of $\Delta p_T/p_T \approx 0.001 p_T$ (p_T in GeV/ c) over the pseudorapidity range $|\eta| < 1.2$. At larger pseu-

dorapidities ($1.2 < |\eta| < 1.4$) tracks are measured with reduced efficiency and momentum resolution. Electromagnetic (EM) and hadronic energies are detected by calorimeters arranged in a projective tower geometry. The central ($|\eta| < 1.1$) EM scintillator calorimeter is 18 radiation lengths (X_0) thick with an energy resolution that scales with transverse energy ($E_T \equiv E \sin \theta$) as $[\sigma(E)/E]^2 = (0.135/E_T^{1/2})^2 + (0.020)^2$. The plug ($1.1 < |\eta| < 2.4$) EM gas calorimeter is $18X_0$ thick at 0° incidence having an energy resolution of $[\sigma(E)/E]^2 = (0.28/\sqrt{E})^2 + (0.02)^2$. An electromagnetic-shower position resolution of several millimeters is obtained in the central region using proportional strip chambers embedded at a depth of $6X_0$ and in the plug using orthogonal readout strips.

Events for this measurement were collected using an inclusive electron trigger. This trigger required a central calorimeter energy cluster with at least 12 GeV of transverse energy and the ratio of hadronic to electromagnetic energy (H/E) to be less than 0.125 and with an associated track in the CTC of transverse momentum $p_T > 6$ GeV/ c . An online hardware processor made the CTC track parameters available at the trigger decision time. The efficiency of this trigger has been studied using data collected at lower trigger thresholds and using W and Z events from independent triggers. We find that this trigger is $(97.3 \pm 0.5)\%$ efficient for $E_T > 15$ GeV. To avoid trigger saturation effects at very high E_T (> 150 GeV), a trigger requiring only a calorimeter energy cluster with $E_T > 60$ GeV was available, ensuring essentially 100% trigger efficiency for such events.

Dielectron events are selected from this sample by making strict requirements on a central (trigger) calorimeter energy cluster while imposing less restrictive criteria for the second electron. The event vertex is required to be within 60 cm (2σ) of the center of the detector along the beam direction. The trigger electron ($E_T > 15$ GeV) selection uses the ratio of H/E and lateral EM shower shape as well as position and momentum matching between the shower and a CTC track. The second electron, detected as a cluster in either the central (CC

event) or plug (CP event) calorimeter, is required to satisfy $E_T > 7$ GeV and is identified on the basis of H/E , VTPC tracking, and lateral shower shape alone. In order to ensure uniform detection efficiency, the clusters are required to be in a fiducial region of the calorimeter. In addition, an isolation requirement is made on both clusters. As a measure of isolation we define $I = (E_C - E_T)/E_C$, where E_C is the total transverse energy within a cone of radius 0.4 in η - ϕ space centered on the cluster (ϕ is the azimuthal angle), and require $I < 0.1$ for both clusters. In order to increase the acceptance for high mass pairs we also accept events where the second electron is identified as an isolated, high- p_T (> 20 GeV/ c) track (CT event). The track is required to extrapolate outside the fiducial region of the calorimeter and is required to be well reconstructed in the CTC by demanding a minimum number of hits in the inner half of the CTC. The track isolation requirement is that the distance in η - ϕ space between the high- p_T track and the nearest track with $p_T > 5$ GeV/ c be greater than 0.4 unit. The isolation requirement for the trigger electron in the event is the same as for the CC and CP events. This sample of isolated dielectron events consists of 156 CC, 145 CP, and 105 CT events.

Efficiencies for the electron identification using calorimetric criteria are derived from the data using Z candidate events (defined by $75 < M < 105$ GeV/ c^2) selected with looser criteria. Our cluster was required to satisfy the trigger electron requirements, allowing efficiencies to be determined with the second electron. The efficiency is measured to be $(88 \pm 2)\%$ for the trigger electron criteria and $(96 \pm 1)\%$ for the second electron criteria in both the central and plug regions, where the errors are statistical only. The systematic uncertainty on these efficiencies is estimated to be 4% by varying the background contribution under the Z peak as measured in sideband regions taken above and below the peak. The track efficiency is measured from W events detected on the basis of an isolated EM cluster and missing-transverse-energy requirements alone. For $|\eta| < 1.2$ this efficiency is measured to be 94%, the small inefficiency being entirely due to the isolation requirement. In the region $1.2 < |\eta| < 1.4$ fewer CTC layers are available for pattern recognition, resulting in a reduced efficiency which we measure to be $(39 \pm 6)\%$. For very-high-energy electrons ($E > 100$ GeV) we expect shower leakage to lower the electron selection efficiency because of the software H/E threshold in the off-line event reconstruction. A parametrization of the H/E cut efficiency as a function of electron energy was determined from the H/E distribution measured with test beam electrons of momenta 50, 100, and 150 GeV/ c . For electrons with $E = 150$ GeV, the H/E cut efficiency is measured to be $(98 \pm 1)\%$. Analysis of the test beam data, extrapolated to 200 GeV, predicts an efficiency of $(92 \pm 3)\%$.

The primary background sources to the Drell-Yan process are dijet and W -jet events where the jets produce

electron candidates passing our identification requirements. Fake electrons are produced from π^\pm, π^0 overlaps and π^\pm undergoing a charge-exchange interaction in the EM calorimeter. Real background electrons result from converted photons originating from π^0 decay and from semileptonic decays of heavy (b, c) quarks. Electron candidates produced in jets are characterized by their relative lack of isolation. We characterize the isolation of the event by the maximum isolation of the two EM clusters (I_{\max}) for CC and CP events, and by the isolation of the trigger cluster for the CT events. A clear signal of isolated events is evident in the distribution of I_{\max} for events satisfying all requirements except isolation [Fig. 1(b)]. In order to extract the magnitude of the background remaining after the isolation requirement ($I_{\max} < 0.1$) this distribution was fitted by a Gaussian (signal) plus polynomial (background) for CC, CP, and CT events separately. The background is assumed to extrapolate to zero at $I_{\max} = 0$. This assumption has been checked with a sample of electrons identified as originating from photon conversions. This method gives 13, 10, and 6 background events in these event classes. We estimate a 10% systematic uncertainty in this background determination. The shape of the invariant mass distribution of the background was determined from the nonisolated ($I_{\max} > 0.1$) pairs with mass greater than 12 GeV/ c^2 . An additional nonisolated background in the CT sample comes from W events where an accompanying jet contains an isolated high- p_T track. This background was estimated to be 4 ± 2 events by using the shape of the track isolation distribution in a sample of W events. A small isolated background from $Z \rightarrow \tau\tau \rightarrow ee$ is also expected. The distri-

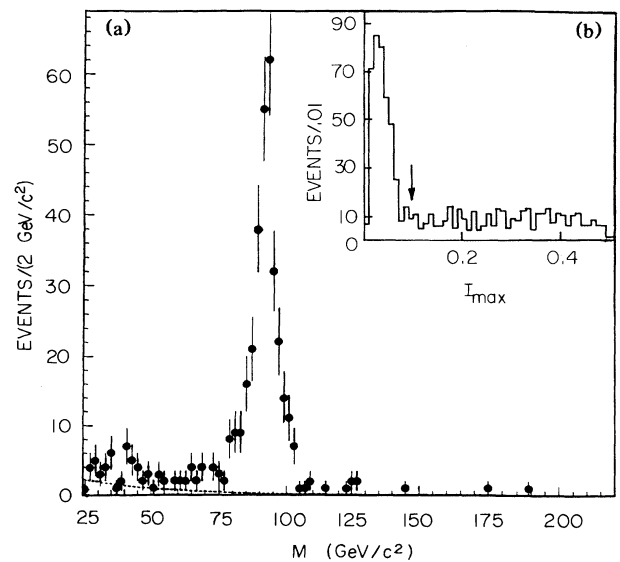


FIG. 1. The mass distribution of isolated pairs is shown in (a) together with the normalized background (dashed line). In the isolation distribution in (b) the signal of isolated pairs is evident near $I_{\max} = 0$. The arrow indicates the location of our cut.

bution in mass of this background was calculated from our Monte Carlo program, and the magnitude (4 ± 1 events) was determined by normalization to the number of observed $Z \rightarrow ee$ events. The normalized background contributions were summed and fitted with a double exponential. The fit is superimposed on the mass distribution of the isolated pairs in Fig. 1(a).

To obtain the cross section, the fitted background was subtracted from the data and the resulting distribution was corrected for all inefficiencies. The total efficiency as a function of electron pair mass was calculated using the ISAJET [6] event generator convoluted with the geometric and kinematic acceptance and detection efficiency. The efficiency falls off sharply at low mass due to the E_T threshold requirements, reaches 38% at the Z mass peak, and flattens to an essentially constant 51% at high mass ($> 200 \text{ GeV}/c^2$) where the events are more centrally produced. QCD effects on the production kinematics are included by initial-state parton evolution in ISAJET. We have checked that the generator adequately reproduces the observed transverse and longitudinal momentum distributions for Z events. We have also checked the relative rates of CC:CP:CT events in the Z mass region which are predicted to be in the ratio 1:1.20:0.80 by our Monte Carlo calculation. The observed ratio is $1:(1.05 \pm 0.14):(0.79 \pm 0.11)$, in good agreement with expectation.

The absolute cross section normalization was obtained from the event rate of the beam-beam counters and a measurement of the effective cross section of these counters by extrapolation from lower-energy measurements [7]. The cross section times branching ratio (σB_Z) for Z production was obtained by summing the differential cross section over a mass range including the Z mass peak and multiplying by a factor calculated from the Monte Carlo program to correct for both the finite integration range and the continuum contribution. Contributions to the systematic uncertainty of this measurement are 4% from selection efficiencies, 2.5% from the effect of the $Z p_T$ -distribution uncertainty on the acceptance correction, 5.0% from the effect of the parton-distribution uncertainty on the acceptance correction, 1.5% from the integration range, $< 1\%$ from the background subtraction, and 6.8% from the luminosity determination. This measurement of σB_Z is in good agreement with our published Z cross section based on an independent analysis [7]. Nine events with $M > 110 \text{ GeV}/c^2$ are observed corresponding to an integrated cross section for $M > 110 \text{ GeV}/c^2$ of $4 \pm 1 \text{ pb}$, consistent with the Drell-Yan expectation of 4 pb.

The shape of the Drell-Yan invariant-mass distribution is most sensitively demonstrated by the integral distribution, $\sigma(M) = \int_M^\infty d\sigma$. The shape of this distribution is compared with a lowest-order Drell-Yan calculation (normalized to the number of observed Z events) in Fig. 2. We have smeared the calculated distribution by a mass-dependent Gaussian resolution function and includ-

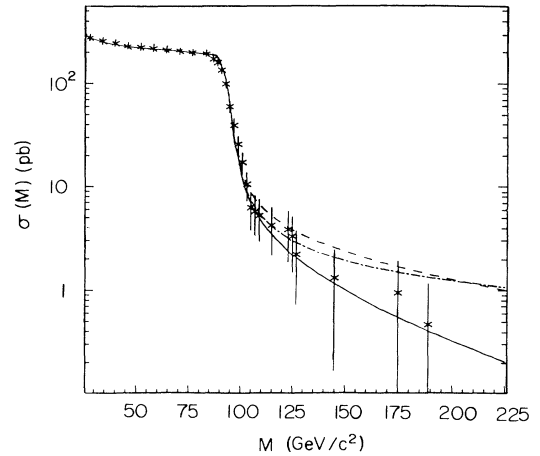


FIG. 2. The integral distribution, $\sigma(M) = \int_M^\infty d\sigma$, as a function of pair mass M . The distribution is compared to a lowest-order Drell-Yan prediction (solid curve). Also shown are the predictions for compositeness scale parameters $\Lambda_{LL} = 2.2 \text{ TeV}$ (dashed line) and $\Lambda_{LL} = 1.7 \text{ TeV}$ (dash-dotted line).

ed the effect of the running of α_s . The excellent agreement even in the low mass region where the background is rising rapidly is a result of the background subtraction. We use the distribution of events above the Z to set a limit on the cross section times branching ratio ($\sigma B_{Z'}$) for additional heavy neutral bosons (Z'). This limit is calculated as a function of Z' mass using the maximum-likelihood technique. The Z' mass distribution was calculated with a width that scales the standard-model Z width by a factor $M_{Z'}/M_Z$. Calculated cross sections are normalized to the observed Z cross section so that systematic errors common to the efficiency and luminosity do not contribute to the limit. The remaining systematic uncertainties are 6% due to the statistical error on the normalization, 1% due to the energy-dependent H/E efficiency, and 2% due to the parton distribution functions and QCD corrections. These have been included in the 95%-confidence-level limit on $\sigma B_{Z'}$ for Z' masses less than $200 \text{ GeV}/c^2$ shown in Fig. 3. Also shown is the theoretical $\sigma B_{Z'}$ calculated with standard-model couplings, normalized to our measured Z cross section.

We expect that high-mass pairs ($M > 200 \text{ GeV}/c^2$) will have a dramatic signature of two isolated high- E_T electrons. We searched for high-mass pairs by relaxing selection criteria on central electrons, requiring only isolation and $H/E < 0.1$. An additional 20 events are observed above the Z peak ($M > 110 \text{ GeV}/c^2$), consistent with a predicted increase in background of 23 events. No additional events are observed above a mass of $200 \text{ GeV}/c^2$. Convoluting the systematic uncertainty of 9.4% with the Poisson limit gives an absolute limit on the observed integral cross section above $200 \text{ GeV}/c^2$ of $\sigma(200) < 1.31 \text{ pb}$ at 95% confidence level. For a Z' with standard-model couplings we exclude $M_{Z'} < 387 \text{ GeV}/c^2$ at 95% confidence level. We can also set a limit on the

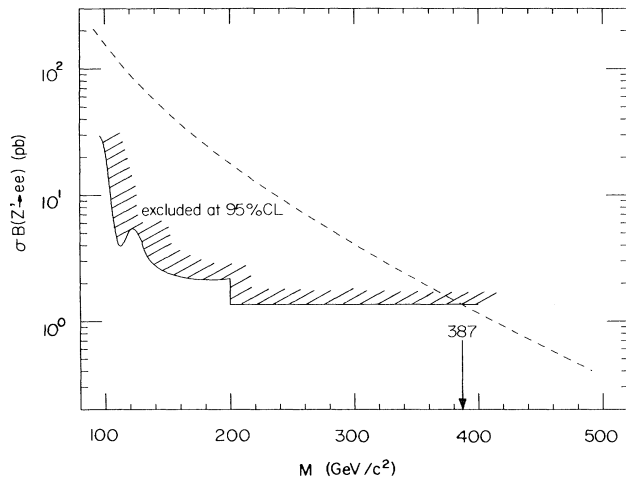


FIG. 3. The 95%-confidence-level limit for $\sigma_{B_{Z'}}$ as a function of $M_{Z'}$, calculated by a maximum-likelihood technique for $M < 200 \text{ GeV}/c^2$ and by the absence of events for $M > 200 \text{ GeV}/c^2$. The shaded region is excluded. The dashed line is $\sigma_{B_{Z'}}$ with standard-model couplings.

scale Λ_{LL}^{\mp} of an effective (contact) lepton-quark interaction which would signal lepton-quark compositeness. The choice \mp corresponds to constructive (destructive) interference with the dominant up-quark contribution to the cross section [8]. Based on the absence of events above a mass of $200 \text{ GeV}/c^2$ we set limits at 95% confidence level of $\Lambda_{LL}^- > 2.2 \text{ TeV}$ and $\Lambda_{LL}^+ > 1.7 \text{ TeV}$. The integral distributions for these values of Λ_{LL}^{\mp} are compared to the observed distribution in Fig. 2.

In conclusion, we have measured the cross section for electron pair production with masses $M > 30 \text{ GeV}/c^2$. We find good agreement between the integrated cross section and the standard-model prediction for the Drell-Yan production mechanism. Based on the distribution of events below $200 \text{ GeV}/c^2$ and the absence of events above $200 \text{ GeV}/c^2$ we set a limit on cross section times branch-

ing ratio for an additional neutral boson. We have checked that this limit is insensitive to variations by a factor of 2 of the Z' width. In addition this limit is independent of the Z' coupling to quarks, making it valid for a large class of models down to masses approaching the Z mass.

We thank the Fermilab Accelerator Division and the CDF technical staff for their effort in the construction and operation of the Tevatron, the Antiproton Source, and this experiment. This work was supported by the Department of Energy, the National Science Foundation, Istituto Nazionale di Fisica Nucleare, the Ministry of Science, Culture, and Education of Japan, and the A. P. Sloan Foundation.

(a)Visitor.

- [1] S. D. Drell and T. M. Yan, Phys. Rev. Lett. **25**, 316 (1970); Ann. Phys. (N.Y.) **66**, 578 (1971).
- [2] A. D. Martin, R. G. Roberts, and W. J. Stirling, Z. Phys. C **42**, 277 (1989).
- [3] See, for example, P. Langacker, R. W. Robinett, and J. L. Rosner, Phys. Rev. D **30**, 1470 (1984); D. London and J. L. Rosner, Phys. Rev. D **34**, 1530 (1986); S. L. Glashow and U. Sarid, Phys. Rev. Lett. **64**, 725 (1990).
- [4] E. Eichten, K. D. Lane, and M. E. Peskin, Phys. Rev. Lett. **50**, 811 (1983).
- [5] F. Abe *et al.*, Nucl. Instrum. Methods Phys. Res., Sect. A **271**, 387 (1988).
- [6] F. Paige and S. Protopopescu, BNL Report No. BNL38034, 1986 (unpublished). We used ISAJET version 6.10.
- [7] F. Abe *et al.*, Phys. Rev. D **44**, 29 (1991).
- [8] The Lagrangian of the contact interaction is taken to be the product of two left-handed color-singlet and isosinglet currents; see Ref. [4]. It has been argued that only the minus sign is theoretically plausible; see M. Suzuki, Phys. Lett. B **220**, 233 (1989).